(2)

AD

TECHNICAL REPORT ARCCB-TR-92038

ENVIRONMENTALLY-CONTROLLED FRACTURE OF AN OVERSTRAINED A723 STEEL THICK-WALLED CYLINDER

J.H. UNDERWOOD
V.J. OLMSTEAD
J.C. ASKEW
A.A. KAPUSTA
G.A. YOUNG

AUGUST 1992

US ARMY ARMAMENT RESEARCH,
DEVELOPMENT AND ENGINEERING CENTER
CLOSE COMBAT ARMAMENTS CENTER
BENÉT LABORATORIES
WATERVLIET, N.Y. 12189-4050

APPROVED FOR PUBLIC RELEASE; DISTRIBUTION UNLIMITED

DISCLAIMER

The findings in this report are not to be construed as an official Department of the Army position unless so designated by other authorized documents.

The use of trade name(s) and/or manufacturer(s) does not constitute an official indorsement or approval.

DESTRUCTION NOTICE

For classified documents, follow the procedures in DoD 5200.22-M, Industrial Security Manual, Section II-19 or DoD 5200.1-R, Information Security Program Regulation, Chapter IX.

For unclassified, limited documents, destroy by any method that will prevent disclosure of contents or reconstruction of the document.

For unclassified, unlimited documents, destroy when the report is no longer needed. Do not return it to the originator.

REPORT DOCUMENTATION PAGE

Form Approved
OMB No. 0704-0188

1. AGENCY USE ONLY (Leave blank)	2. REPORT DATE	3. REPORT TYPE AND DATES COVERED
	August 1992	Final

4. TITLE AND SUBTITLE
ENVIRONMENTALLY-CONTROLLED FRACTURE OF AN OVERSTRAINED A723 STEEL THICK-WALLED CYLINDER

5. FUNDING NUMBERS
AMCMS: 6126.24.H180.0

6. AUTHOR(S)
J.H. Underwood, V.J. Olmstead, J.C. Askew, A.A. Kapusta, and G.A. Young

7. PERFORMING ORGANIZATION NAME(S) AND ADDRESS(ES)
U.S. Army ARDEC
Benet Laboratories, SMCAR-CCB-TL
Watervliet, NY 12189-4050

8. PERFORMING ORGANIZATION REPORT NUMBER
ARCCB-TR-92038

9. SPONSORING / MONITORING AGENCY NAME(S) AND ADDRESS(ES)
U.S. Army ARDEC
Close Combat Armaments Center
Picatinny Arsenal, NJ 07806-5000

10. SPONSORING / MONITORING AGENCY REPORT NUMBER

11. SUPPLEMENTARY NOTES
Presented at the Twenty-Third Symposium on Fracture Mechanics, College Station, Texas, 18-20 June 1991. Published in: *Fracture Mechanics, Twenty-Third Symposium*

12a. DISTRIBUTION / AVAILABILITY STATEMENT
Approved for public release; distribution unlimited

12b. DISTRIBUTION CODE

13. ABSTRACT *(Maximum 200 words)*

A through-wall, 1.7-m long crack grew suddenly from a notch in a 285-mm outer diameter (OD) of an A723 steel overstrained tube that was undergoing plating operations with no externally applied loads. The fracture mechanics tests and analyses and the fractography performed to characterize the cracking are described in this report. The tube had a yield strength of 1200 MPa, fracture toughness of 150 MPa$\sqrt{m}$, and a tensile residual stress at the OD of about 600 MPa. The composition was typical of an air-melt A723 steel, and the electropolishing bath, consisting of sulfuric and phosphoric acids, was held at 54°C.

The bolt-loaded test for the threshold stress intensity factor for environmentally-controlled cracking described by Wei and Novak was used here with two significant modifications. Some tests included only a notch with the radius matching that of the tube, and a new expression for K in terms of crack-mouth displacement was developed and used. Scanning electron microscope fractography and energy dispersive x-ray spectra were used to identify crack mechanisms.

Results of the investigation include: (a) a measured threshold of hydrogen stress cracking for the material/environment below 20 MPa$\sqrt{m}$; (b) da/dt versus K behavior typical of classic environmental control; and (c) an improved K/v expression for the bolt-loaded specimen and associated criteria for determining plane-strain test conditions in relation to the Irwin plastic zone.

14. SUBJECT TERMS	15. NUMBER OF PAGES
Environmental Cracking, Test Methods, Hydrogen Stress Cracking, Thick-Walled Cylinder, K Analysis, Scanning Electron Microscopy, Residual Stress	26
	16. PRICE CODE

17. SECURITY CLASSIFICATION OF REPORT	18. SECURITY CLASSIFICATION OF THIS PAGE	19. SECURITY CLASSIFICATION OF ABSTRACT	20. LIMITATION OF ABSTRACT
UNCLASSIFIED	UNCLASSIFIED	UNCLASSIFIED	UL

TABLE OF CONTENTS

TABLES

LIST OF ILLUSTRATIONS

ACKNOWLEDGMENTS

We are pleased to credit the following people from Benet Laboratories: Mr. J. Zalinka and Mr. D. Corrigan for performing mechanical and fracture testing and Mr. C. Rickard for optical measurements and fractography.

INTRODUCTION

'Postmortem' studies of crack growth-induced structural failure are often prompted by an unanticipated failure that also has economic significance. Such is the case here. In August 1990, a nearly finished cannon tube suffered an unexpected and complete failure. A crack grew from a notch in the 285-mm outer diameter (OD) of the tube, down the tube axis for 1.7 m, and through to the 157-mm inner diameter (ID) over most of the 1.7-m length, thereby ruining the tube. Figure 1 shows some aspects of the configuration. At the time of the failure, the tube was being chromium plated with no externally applied mechanical loads. The plating baths were above the tube ambient temperature, which can result in applied transient thermal stress, but as shown in the upcoming analysis, these thermal stresses were of a level too low to have been a primary cause of the failure. The unique residual stress state of the tube was considered from the start to be a significant factor in the failure. Prior work (ref 1) showed the important and deleterious effects of overstrain residual stresses on crack growth from a similar notch and tube configuration. However, unlike the previous work that involved fatigue loading, this failure involved only the sustained loads due to overstrain residual stresses and the low level thermal stresses mentioned previously. Thus, environmentally-controlled cracking was the suspected cause of the failure, particularly upon consideration of the acids commonly used in plating operations.

OBJECTIVE

The objective of this report is to describe the tests and analyses used to identify the specific cause of the cracking and related failure and to describe both the overall macrofailure process of the tube as a structure, as well as the micromechanisms of the cracking that led to the failure. As the investigation proceeded, some of the available fracture test and analysis methods from the technical literature were modified in order to broaden their usefulness or improve their accuracy. Thus, a secondary objective of the work became the development of modified and new test and analysis procedures for use in the investigation and for general use in fracture testing.

MATERIAL AND ENVIRONMENTS

The tube that failed was machined from an A723 steel forging with mechanical properties and chemical analysis as shown in Table 1. The tensile and fracture test results were the mean of two circumferential orientation samples from a location near the failure. The circumferential orientation is critical in most pressurized tubes and was the orientation of the failure (see Figure 1). The chemical analysis was from direct reading emission spectrometer results from specimens near the failure location. In general, the Table 1 results meet the requirements of A723, Grade 1, Class 4. The only exceptions are the molybdenum content of 0.51 percent, which is somewhat above the 0.40 percent upper limit of Grade 1, and the Charpy energy of 25 J at -40°C, which is not the same as the 27 J at +5°C requirement of Class 4. However, these differences are not considered significant. There appears to be no deficiency with the tube based on material properties.

The chemical baths used with the tube are those typically used in chromium plating: sodium hydroxide in water for electrocleaning; concentrated sulfuric acid + phosphoric acid for electropolishing; chromic acid + sulfuric acid in water for plating; sodium hydroxide in water for stripping of the plated chromium, if necessary. The prime suspect environment for this failure was the electropolish bath, because it was a mixture of concentrated acids including sulfuric acid, which is known to be highly aggressive toward steels. The concentrations and test temperatures used for the electropolish solution with the tube (and the subsequent modeling tests) are given in Table 1.

Table 1. Properties of Steel and Chemical Environment

A723 Steel:

Mechanical Properties	Yield Strength	Tensile Strength	Charpy Energy	Fracture Toughness
	(circumferential)		(C-R orientation)	
Measured	1207 MPa	1282 MPa	25 J -40°C	157 MPa $m^{1/2}$ +20°C
Specified	1105 MPa min	1205 MPa min	27 J +5°C	-

Chemical Analysis (wt.%):

	C	Mn	Mo	Si	Cr	Ni	V	P	S
Measured	0.33	0.60	0.51	0.13	1.03	2.11	0.11	0.010	0.009
Specified	0.35 max	0.90 max	0.40 max	0.35 max	0.80-2.00	1.50-2.25	0.20 max	0.015 max	0.015 max

Acid Solution:

Concentrated H_2SO_4 (98 wt.%)	Concentrated H_3PO_4 (85 wt.%)	Test Temperature	
		Cylinder	Specimens
50 vol %	50 vol %	54°C	20-54°C

FAILURE DETAILS AND MODELING TESTS

The tube was subjected to the plating baths mentioned previously, including the stripping bath, which was required to remove uneven plating products. The sequence of baths was repeated, and the failure was noted as the tube was removed from the stripping bath, which was again required to remove uneven plating. The fact that the failure was noted following exposure to the sodium hydroxide stripping bath placed the initial attention on this environment. However, attention quickly shifted to the sulfuric acid + phosphoric acid environment, because the latter is so much more aggressive. The electrolytic cleaning, polishing, plating, and stripping operations were performed with an electrode inserted in the ID of the tube and with the entire tube subjected to the baths. Therefore, the failure, which was initiated at the OD of the tube, was considered to be controlled by chemical environment and not by any electrochemical process.

The crack extended 1.7 m along the tube axis and into the ID surface, as mentioned previously. It initiated from and was guided by a 9.8-mm deep, 24-mm wide, 1.7-m long notch in the OD surface, (shown schematically in Figure 1) with a notch root radii of 1.1 mm. The maximum opening of the crack at the notch root was 11.7 mm at a location about midway along the 1.7-m length of the crack. The fracture surface was removed and examined and showed two distinct regions. The first was a dark colored region

emanating from one of the notch roots near the middle of the 1.7-m long overall fracture surface and is believed to be an area of environmentally-controlled fracture. This region was generally covered with a corrosion product and had a length of 430 mm, an average depth (from the notch root) of 5.6 mm, and a maximum depth of 11.9 mm. The corrosion-covered region included two distinct areas, one near the notch root having thinner, more uniform and adherent corrosion, and an area further from the notch having darker, thicker, and more brittle and porous corrosion. The nature of these two areas is consistent with the two complete plating cycles that were applied, with the second cycle removing some of the corrosion product near the notch. The second region of the fracture surface had no corrosion and made up the remainder of the fracture surface. It is believed to be an area of fast fracture.

To be sure that the understanding of the failure was correct--residual stress and the presence of the acids caused environmental cracking that led to fast cracking--the following modeling tests and analyses were performed. Environmental cracking threshold tests and plane-strain fracture toughness tests were performed using samples of the failed tube and samples of the acid bath used to electropolish the tube. Scanning electron microscope (SEM) fractographs and energy dispersive x-ray spectra of the tube fracture surface were compared with similar results from the controlled laboratory tests. Stress intensity factor relations were developed for the tube configuration and residual stress conditions, and comparisons were made between the experimental and analytical results.

The following sections of this report describe the tests and analyses and their results and implications.

TEST PROCEDURES

The most important test results required to model and understand the tube failure are a demonstration of environmental cracking in the suspect environment and a measurement of a threshold K value for cracking. Bolt-loaded specimens have clear advantages of simplicity for environmental testing, and the work of Wei and Novak (ref 2) provides a comprehensive basis for this type of test. Reference 2 describes a bolt-loaded compact specimen with generic 'arm' height-to-depth ratio, H/W, of 0.486 and the detailed test procedures for environmental cracking tests with this specimen. Figure 2 shows the specimen used here, as suggested in Reference 2.

Several aspects of the Wei and Novak procedure for environmental cracking tests should be emphasized. One recommendation found to be critical in interlaboratory tests of environmentally-assisted cracking (ref 2) is believed to be equally important in these tests, that is, the application of the test environment before the application of the load. As shown by the test results, if this recommendation had not been followed, the fast environmental cracking may not have been observed, and it was this fast cracking that led to the failure of the tube. The recommendation to apply environment before load allows breakage of protective layers at the notch tip and thereby exposure to the environment of fresh metal, a mechanism often proposed for environmental cracking.

Two aspects of the procedure (ref 2) were modified in the tests here. First, in two of the tests the usual fatigue precrack was omitted in order to duplicate the 1.1-mm notch root radius of the tube that failed. Other tests used a precrack, as shown in Table 2. A second modification of the Wei and Novak procedures was the development and use of a different expression for the ratio of applied stress intensity to applied crack-mouth opening, K/v. The expression from Reference 2 is

$$KW^{1/2}(a/W)^{1/2}/Ev = f_1(a/W) / f_2(a/W) \quad (1)$$

$$f_1 = 30.96(a/W) - 195.8(a/W)^2 + 730.6(a/W)^3 - 1186.3(a/W)^4 + 754.6(a/W)^5$$

$$f_2 = \exp[4.495 - 16.130(a/W) + 63.838(a/W)^2 - 89.125(a/W)^3 + 46.815(a/W)^4]$$

for $X/W = 0.255$; $H/W = 0.486$; $0.3 \geq a/W \geq 0.8$

where E is elastic modulus and the other symbols are defined in Figure 2. Equation (1) was fitted to reliable numerical results (ref 3), but it is relatively complex, and (as stated in Reference 2) "there are uncertainties associated with the K calibration which have not been fully addressed." Therefore, a different K expression was developed, as shown in Figure 3. A much lower order polynomial was used to fit a parameter that included the ratio K/v, of prime importance for the bolt-loaded compact specimen, but also included the functional form of the deep crack limit of K/v for the specimen. This limit can be obtained from two limit solutions for the remotely applied moment, M, available from Tada, Paris and Irwin (ref 4) in a manner similar to that from prior work (ref 5)

$$\lim_{a \to W} K = 3.975\ M/B\ (W-a)^{1/2} \quad (2)$$

$$\lim_{a \to W} \theta = 15.8\ M/EB\ (W-a)^2 \quad (3)$$

combined with the limit relation for crack opening angle, θ,

$$\lim_{a \to W} \theta = v/(W + x) \quad (4)$$

The general result for compact specimens (independent of H/W) is

$$\lim_{a \to W} [KW^{1/2}/Ev(1 - a/W)^{1/2}] = 0.2516/(1 + X/W) \quad (5)$$

and for the $X/W = 0.255$ of interest here,

$$\lim_{a \to W} [KW^{1/2}/Ev(1 - a/W)^{1/2}] = 0.2005 \quad (6)$$

This is the limit shown in Figure 3 and used in a cubic polynomial fit, resulting in the following K/v expression

$$KW^{1/2}/Ev(1-a/W)^{1/2} = 0.654 - 1.88(a/W) + 2.66(a/W)^2 - 1.233(a/W)^3 \quad (7)$$

for $X/W = 0.255$; $H/W = 0.486$; $0.3 \geq a/W \geq 1.0$

This expression fits the numerical results of Newman (ref 3) over the range $0.3 \geq a/W \geq 0.8$ within 0.6 percent and the deep crack limit within 0.2 percent. Note that the fit of the Wei and Novak expression to Newman's results is not as good. Also, for $a/W > 0.8$, crack lengths of importance in these tests and in general for displacement-loaded compact specimens, the Wei and Novak expression does not

approach the deep crack limit. Equation (7) was used for all calculations of applied K in the bolt-loaded tests.

Table 2. Specimens and Test Conditions

Test #	Notch Conditions		Initial Load Application			Test Duration Hours
	a_o/W	Precrack	In	v_o, mm	K_o, MPa√m	
3	0.39	none	air	0.62	100	120
10	0.45	2 mm	acid	0.70	114	4
7	0.44	2 mm	acid	0.66	110	2400
15	0.44	2 mm	acid	0.50	82	1540
16	0.44	2 mm	acid	0.33	54	1540
17	0.40	none	acid	0.93	168	0.1

Two K_{Ic} tests were conducted using the arc tension specimen of ASTM Test for Plane-Strain Fracture Toughness of Metallic Materials (E-399) with thickness B = 38 mm. The results, 156 and 159 Mpa√m, had a mean K_{max}/K_{Ic} value of 1.03, well within the 1.10 requirement, but had a mean 2.5 $(K_{Ic}/\sigma_{ys})^2$ value of 43 mm, somewhat larger than B. Since only one of these basic test requirements was not met, and by a relatively small margin, the test results are believed to give a good measure of fracture toughness.

Referring again to Table 2, the general test procedure was to precrack (except for specimens #3 and #17) at a maximum K of about 50 MPa√m, apply a few drops of the acid solution at laboratory ambient temperature (20°C) and immediately (within one minute) apply an initial displacement, v_o, and then immerse (within about five minutes) in the acid solution held at a temperature of 54°C. The total test durations are listed in Table 2. The mean crack depth was determined from microscopic measurements on both surfaces with various inspection frequencies. The first sample listed in the table (#3) was not subjected to the few drops of acid solution before load application. As discussed in the next section, the results were quite different.

RESULTS AND DISCUSSION

Least Severe Model Test

Of the six specimens tested, the first, #3, had a notch the same radius as the tube, no precrack, and was loaded in air to K_o = 100 MPa√m. These test conditions were intended to model the least severe conditions that could have been present in the tube, that is, no sharpening of the notch and no acid present as the stress was applied. The K_o value of 100 MPa√m was selected based on the following. The circumferential direction residual stress, σ_R, at the tube OD was calculated using (ref 6)

$$\sigma_R/\sigma_{ys} = 1 - 2\ln(\beta/\delta) / [(\beta/\delta)^2 - 1] \quad (8)$$

where β and δ are the outer and inner radii of the tube, as shown in Figure 1. Equation (8) gives the stress for a 100 percent overstrained tube, that is, one in which the plastic straining has proceeded completely through the tube wall due to the application of overpressure or mandrel expansion to the tube. The failed tube was 100 percent overstrained, as verified by a destructive slitting test of a ring from the tube. The result from Eq. (8), σ_R = 576 MPa, used with the expression for K for a short edge crack under

remote tension

$$K_R = 1.12\,\sigma_R\,(\pi a)^{1/2} \qquad (9)$$

gives a calculated value of K_R = 114 MPa√m for a 9.8-mm deep notch. This value may be only an estimate of the effective K in the tube because Eq. (9) assumes a sharp crack, the tube contained a notch, and because the eq ation ignores the stress gradient through the tube wall. Nevertheless, Eq. (9) does give a reasonable estimate of K for a cracked tube with residual stress, based on the following comparison of K_R with K_{Ic}. Using σ_R = 578 MPa, as before, and the average and maximum total crack depths, 15.4 and 21.7 mm, gives K_R values of 142 and 169 MPa√m, respectively, which bracket the measured K_{Ic}, 157 MPa√m. Note that in these calculations, a is the total depth of the notch (9.8 mm) plus the crack depth.

The results of the specimen #3 test of the least severe conditions that could have been present in the tube were essentially negative. Although small cracks were noted in the disturbed area near the machined surfaces of the notch, no crack growth was observed by optical or electron microscopic examination following 120 hours of acid exposure at 54°C. This indicates that the conditions were more severe in the failed tube. Although no large inclusions were noted on the tube fracture surface, manganese sulfide inclusions are always present to some extent in this type of steel and could have effectively sharpened the notch.

Precracked Tests

The next four specimens were precracked (about 2-mm extension of notch), subjected to a few drops of acid, and then loaded: two specimens to a high load, which corresponded to the tube loading, and one each to an intermediate and low load. The high load tests had dramatically different results than test #3. Cracking was noted almost immediately upon loading of specimens #10 and #7; about five minutes after applying drops of acid to the notch and crack area and about three minutes after applying the load, several millimeters of crack growth could be seen with the unaided eye on both sides of the specimen. The tests were continued in the 54°C acid bath as described previously; test #10 was ended at 4 hours, in an attempt to obtain a fracture surface relatively unaffected by corrosion products, and test #7 continued for 2400 hours to obtain a threshold K for cracking in this environment.

Figure 4 is a plot of crack depth and applied K versus exposure time for the two high load precracked tests. The fast "three minute" cracking noted earlier occurred very near the left ordinate; for specimen #7, the first two points show crack growth from 21 mm (the total depth of notch plus precrack) to 28 mm, while K changes from K_o = 110 MPa√m to K = 88 MPa√m after 0.05 hour of exposure. This "three minute" cracking is followed by a region of steadily increasing crack depth and decreasing K, and finally by a region of relatively constant crack depth and K.

The nature of the cracking in this tube is essentially the same as hydrogen stress cracking described by Uhlig and Revie (ref 7). They describe cracking of martensitic steels that occurs within a few minutes upon exposure to acid solutions and an applied or residual tensile stress. All of these conditions are met in the case of this cylinder, and, as already noted, both the acid environment and the tensile stress are particularly severe.

The three regions of behavior in Figure 4 can be explained by a plot of crack growth rate versus applied K, as seen in Figure 5. A five-point floating average procedure was used to calculate da/dt, in a manner similar to the secant method of ASTM Test for Constant-Load-Amplitude Fatigue Crack Rates Above 10^{-6} m/Cycle (E-647). The crack depth and time values for the n+2 and the n-2 data points were used to calculate $\Delta a/\Delta t$, which was plotted versus K of the middle data point set of five. If the n+1 and n-1 data points had been used in Figure 5, the result would have been similar but with more scatter. It is interesting to note the similarity of the trend of the data with the classic three regions of environmental

crack growth rate behavior (ref 7): region I at low K, approaching a threshold; region II at intermediate K and a constant da/dt; region III at high K, approaching the critical K for fast fracture. This similarity to the classic behavior gives further verification that environmental effects controlled the tube failure.

Figures 6 and 7 compare results of crack depth and applied K versus exposure time for three levels of initial load, K_o. The intermediate and low initial K_o tests, #15 and #16, respectively, showed no initial fast cracking, but otherwise the three sets of results were generally similar. Note in Figure 7 that the applied K after about 1500 hours of exposure approached a relatively constant K value for very deep cracks in the three tests. These results are a useful measurement of a threshold K for cracking for these tests and are summarized in Table 3. One of the three tests (#7) was continued further to a total of 2404 hours of exposure. There was no significant change in a/W (still 0.98) or applied K (18.0 MPa$\sqrt{m}$).

Table 3. 1540-Hour Threshold Values of K for A723 Steel in H_2SO_4 + H_3PO_4 Environment at 54°C

Test #	Crack Depth a/W	Initial Load K_o, MPa$\sqrt{m}$	Test Duration Hours	Threshold K_{th}, MPa$\sqrt{m}$
7	0.98	110	1588	18.6
15	0.96	82	1540	19.0
16	0.94	54	1540	16.2
				mean: 17.9
				std dev: 1.5

Plane-Strain Limit

One aspect of concern in the apparent threshold values discussed in Figure 7 and Table 3 was the notably deep cracks in the tests. Even though the expression used to calculate K, Eq. (7), was accurate for a/W → 1, there is still the concern that the Irwin plastic zone may become significant in size relative to the remaining uncracked ligament as a/W → 1. If this occurred, the threshold values would be suspect due to loss of plane-strain constraint. The following analysis was performed to develop specimen size and crack depth criteria for the displacement-loaded compact specimen that would ensure plastic zones small enough to maintain plane-strain conditions. Starting with the relation for adequate specimen size relative to plastic zone size used in ASTM Test E-399

$$(W\text{-}a) \geq 2.5(K_{Io}/\sigma_Y)^2 \qquad (10)$$

and combining Eq. (10) with Eq. (5), gives an expression for a dimensionless factor that defines the ratio of v_o to W required for plane-strain conditions

$$\tau_{Ic} = Ev_o/\sigma_{ys}W \leq 2.51\,(1 + X/W) \qquad (11)$$

For a material with given values of σ_{ys} and E, if the factor, which could be called a plane-strain limit factor, τ_{Ic} is less than the specified value, then the test results are valid with respect to plastic zone size. Note the simplicity of the expression, particularly that valid results can be predicted for the deepest of cracks. However, considering the similar form of Eqs. (5) and (10), specifically the fact that (W-a) varies as K_I^2 in both expressions, the simple result is not surprising. A physical interpretation is that the plastic zone size and the remaining ligament size have a constant ratio for the displacement-loaded specimen.

Therefore, for cracks deep enough that the limit solution of Eq. (5) controls K/v, Eq. (11) can be used and cracks of any depth can give valid results. It is clear from the nearly constant values in Figure 3 for $0.6 \leq a/W \leq 1$ that the limit solution controls K/v over this range.

Expressions for the plane-strain limit factor for two commonly used displacement-loaded specimens follow directly from Eq. (11). For the bolt-loaded compact specimen, the expression is

$$\tau_{1c} = Ev_o/\sigma_{ys}W \leq 3.15 \qquad \text{for } X/W = 0.255 \tag{12}$$

Referring to Table 2, the first five tests listed met this criterion, which includes all the tests with deep cracks. For the wedge-loaded compact specimen of ASTM Test for Plane-Strain Crack-Arrest Fracture Toughness, K_{Ia}, of Ferritic Steels (E-1221), the expression is

$$\tau_{1c} = Ev_o/\sigma_{ys}W \leq 3.14 \qquad \text{for } X/W = 0.250 \tag{13}$$

Notched Test and Thermal Stress

One further crack growth test was performed: #17 listed in Table 2. The sample had the 1.1-mm radius notch with no precrack, was subjected to acid in the notch (at 20°C), and then bolt-loaded to a v_o about 50 percent higher than #3. Since specimen #3 had shown no crack growth from a notch when loading preceded the application of the acid, this further test explored the application of acid before loading and when loading to a higher level. The displacement was increased gradually so that K increased from 100 to 168 MPa$\sqrt{m}$ in about two minutes, whereupon cracking began. After about three minutes, the crack grew 16 mm, and the specimen was broken apart for fracture surface examination.

The results of specimen #17 suggest that a precrack is not required for fast environmental cracking in this material and environment, but environmental contact before loading does seem to be required. A question arises as to a source of loading in the tube that would have occurred after contact with the acid. The following answer is proposed. Transient thermal stresses caused by the sudden entry of the tube into the hot acid would reach their maximum level several seconds after entry of the tube. The magnitude of these stresses can be approximated by the steady state stresses in a tube with the OD held at the higher temperature, 54°C, and the ID at ambient temperature, 20°C. An expression for the stress at the tube OD under these conditions (ref 8) and concentrated by the stress concentration factor, k, of the notch is

$$\sigma_T = k\Delta T\alpha E[1 - 2\ln(\beta/\delta)/(\beta^2/\delta^2 - 1)]/[2(1-\mu)\ln(\beta/\delta)] \tag{14}$$

Using Eq. (14) with $\Delta T = 34$°C, $k = 6$ from prior work (ref 1), $\alpha = 12$/°C (ref 9), and Poisson's ratio, $\mu = 0.3$, a compressive thermal stress at the notch tip of 293 MPa is predicted. If the effect of the loading following environmental contact is to break brittle protective films and thereby expose fresh metal to the acid, it should not matter whether the stress is compressive or tensile, particularly when it is concentrated at the notch tip. Following this reasoning, thermal loading could have provided the critical loading that followed the acid contact in the tube failure process.

Fractography and Spectra

This final section gives fractographic results corresponding to some of the crack growth results already presented. The objective was to corroborate (or refute) the belief that hydrogen stress cracking was the cause of the tube failure and to show other important features of the tests.

Figure 8 shows low magnification views of two fracture surfaces with corrosion products present. In the optical photo, Figure 8(a), the corrosion did not obscure the area near the fatigue precrack

(bottom) nor the area near the last ligament, which was broken in air after removal from the acid (top), both of which showed that the crack front was quite straight. The light shaded corrosion product has the appearance of a non-straight crack front, but careful examination showed the crack was straight in this area as well. A straight crack is an important requirement for the deep crack tests here, in complement to the proposed K/v expression and plane-strain requirements already discussed. The SEM photo, Figure 8(b), is a portion of the fatigue precrack (bottom) and the subsequent environmental crack. Secondary cracking can be seen in the environmentally affected area of the fracture surface.

A few areas could be found on the environmental cracking fracture surfaces that were relatively free of corrosion products. Figure 9 shows high magnification SEM fractographs that compare a corrosion-free product area from the tube with an area ahead of the environmental cracking. Figure 9(a), from an area just ahead of the notch, shows areas of secondary cracking and intergranular cracking, both of which have been associated with environmental cracking.

Evidence of manganese sulfide stringers is also clear, aligned with the tube axis (horizontal in the photo). Immediately ahead of the area of environmental cracking, the appearance is typical dimpled rupture, as expected for fast, K_{Ic}-type fracture, as seen in Figure 9(b). Figure 10 shows relatively corrosion-free areas of two specimens believed to be areas of environmental cracking, and the clear indications of secondary cracking and intergranular cracking confirm this belief. Note the similarity of the fracture appearance in the modeling specimens of Figure 11 and that from the tube in Figure 9(a).

Energy dispersive x-ray spectra were taken at many of the areas of SEM study. Figure 11 presents the key results from areas believed to be due to environmental cracking: two from the failed tube and two from a test specimen. The results were obtained using a relatively low voltage for this process, 10 kV, in order to focus more on the surface layers of the sample than on the metal substrate. Spectra (a) and (b) are from the tube in areas comparatively free of corrosion and covered with corrosion, respectively (spectrum (a) is from near the area of the SEM photo of Figure 9(a)). In spectrum (a), the sulfur and phosphorous indications are consistent with the sulfuric and phosphoric acid mixture being the cause of the cracking. Spectrum (b) is consistent with the presence of all the chemicals applied to the tube, which were sulfuric acid, phosphoric acid, sodium hydroxide, and chromic acid. This indicates that identification of the most obvious and heavy corrosion product does not necessarily identify the specific cause of cracking.

Spectra (c) and (d) are from specimen #10 in areas comparatively corrosion-free and covered with corrosion, respectively (spectrum (c) is from near the area of the SEM photo of Figure 10(a)). In spectrum (c), a phosphorous indication can be seen, and perhaps a sulfur indication, although it has not been designated. Spectrum (d), of a heavy corrosion area, includes clear indications of phosphorus, sulfur, and oxygen. The presence of oxygen is evidence that the corrosion product includes an oxide of sulfur, phosphorous, or perhaps iron.

Implications

The results suggest, as in any study of environmental cracking, that cracking could be avoided by eliminating the aggressive environment or by eliminating or reducing the tensile stress. Neither the acid nor the residual stress could be eliminated without significant changes in the design and manufacturing process of the component. However, the concentration of the stress by the notch can be reduced with relatively little bother. Referring to a compendium of stress concentration factors (ref 10), if the 9.8-mm depth of the notch remained the same and the notch radii were increased to a significant portion of the depth, say 8 mm, the result would be a k = 2.16. Thus, by replacing the nearly square cornered notch with one approaching a semicircle, the maximum stress would reduce to 36 percent of its former value. This would significantly reduce the likelihood of environmental cracking and failure of the tube by reducing both the concentrated residual stress, which initiates and drives the cracking, and the thermal

stress, which may accelerate the initiation process. An added bonus would be improved nondestructive inspection access to cracking, should it occur.

SUMMARY AND CONCLUSIONS

The following are the key results and conclusions of the work regarding the environmental cracking in the tube and the associated modeling tests:

1. Hydrogen stress cracking was identified as the cause of the tube cracking and was modeled in bolt-loaded compact specimen tests of the same material and environment. Overstrain residual stress, concentrated at an OD notch, provided the sustained tensile stress; a mixture of concentrated sulfuric and phosphoric acids at 54°C was the aggressive environment.

2. Modeling tests showed fast environmentally-controlled cracking, with several millimeters of growth occurring typically in three minutes at applied K levels above 80 MPa$\sqrt{m}$. A threshold of environmental cracking was observed following 1540 hours of acid exposure; three tests at different initial K levels resulted in threshold values of 16 to 19 MPa$\sqrt{m}$. A da/dt versus K plot of results showed the classic phase I-III environmental cracking behavior.

3. Scanning electron microscope fractography and energy dispersive x-ray spectra of tube and model specimen fracture surfaces corroborated the fracture mechanics test results. Secondary cracking and intergranular cracking were observed in the few areas of the fracture surface not obscured by corrosion product. Spectra of the tube and modeling surfaces showed clear sulfur and phosphorous indications in the areas in which secondary and intergranular cracking were observed.

4. Thermal stresses concentrated by the notch were proposed as the source of the critical loading that followed environmental contact and broke the protective layers, and thereby accelerated the environmental cracking of the tube.

The following are the key results regarding the development of new test and analysis procedures for environmental cracking studies:

1. A new K expression was developed for the H/W = 0.486 bolt-loaded specimen that is simpler, a better fit to Newman's numerical results, and fits a wider range of a/W, including the deep crack limit solution for this specimen.

2. A new criterion was developed for the specimen size required to maintain plane-strain constraint for displacement-loaded compact specimens. The similar form of the relationships for the Irwin plastic zone and the K limit for the specimen resulted in a simple size criterion.

3. A floating five-point average da/dt calculation procedure gave a good description of environmental crack growth for a bolt-loaded specimen.

REFERENCES

1. J.A. Kapp and J.H. Underwood, "Service Simulation Tests to Determine the Fatigue Life of Outside-Diameter-Notched Thick-Wall Cylinders," *Experimental Mechanics*, Vol. 22, No. 3, March 1982, pp. 96-100.

2. R.P. Wei and S.R. Novak, "Interlaboratory Evaluation of $K_{t_{th}}$ and da/dt Determination Procedures for High-Strength Steels," *Journal of Testing and Evaluation*, Vol. 15, No. 1, January 1987, pp. 38-75.

3. L.A. James, "Compliance Relationships for the WOL Specimen Revisited," report to ASTM Subcommittee E-24.04 on Subcritical Crack Growth, July 1989.

4. H. Tada, P.C. Paris, and G.R. Irwin, *The Stress Analysis of Cracks Handbook*, Paris Productions Inc., St. Louis, MO, 1985, p. 9.1.

5. J.H. Underwood, I.A. Burch, and J.C. Ritter, "Crack-Arrest and Static Fracture Toughness Tests of a Ship Plate Steel," *Rapid Load Fracture Testing, ASTM STP 1130*, American Society for Testing and Materials, Philadelphia, 1992, pp. 147-160.

6. T.E. Davidson, C.S. Barton, A.N. Reiner, and D.P. Kendall, "Overstrain of High Strength Open End Cylinders of Intermediate Diameter Ratio," *Proceedings of the First International Congress on Experimental Mechanics*, Pergamon Press, Oxford, 1963.

7. H.H. Uhlig and R.W. Revie, *Corrosion and Corrosion Control*, Wiley, New York, 1985, pp. 123-147.

8. R.J. Roark and W.C. Young, *Formulas for Stress and Strain*, McGraw-Hill, New York, 1975, pp. 582-587.

9. C.J. Smithells, *Metals Reference Book*, Butterworths, Washington, 1962, pp. 705-711.

10. R.E. Peterson, *Stress Concentration Factors*, Wiley, New York, 1974, p. 40.

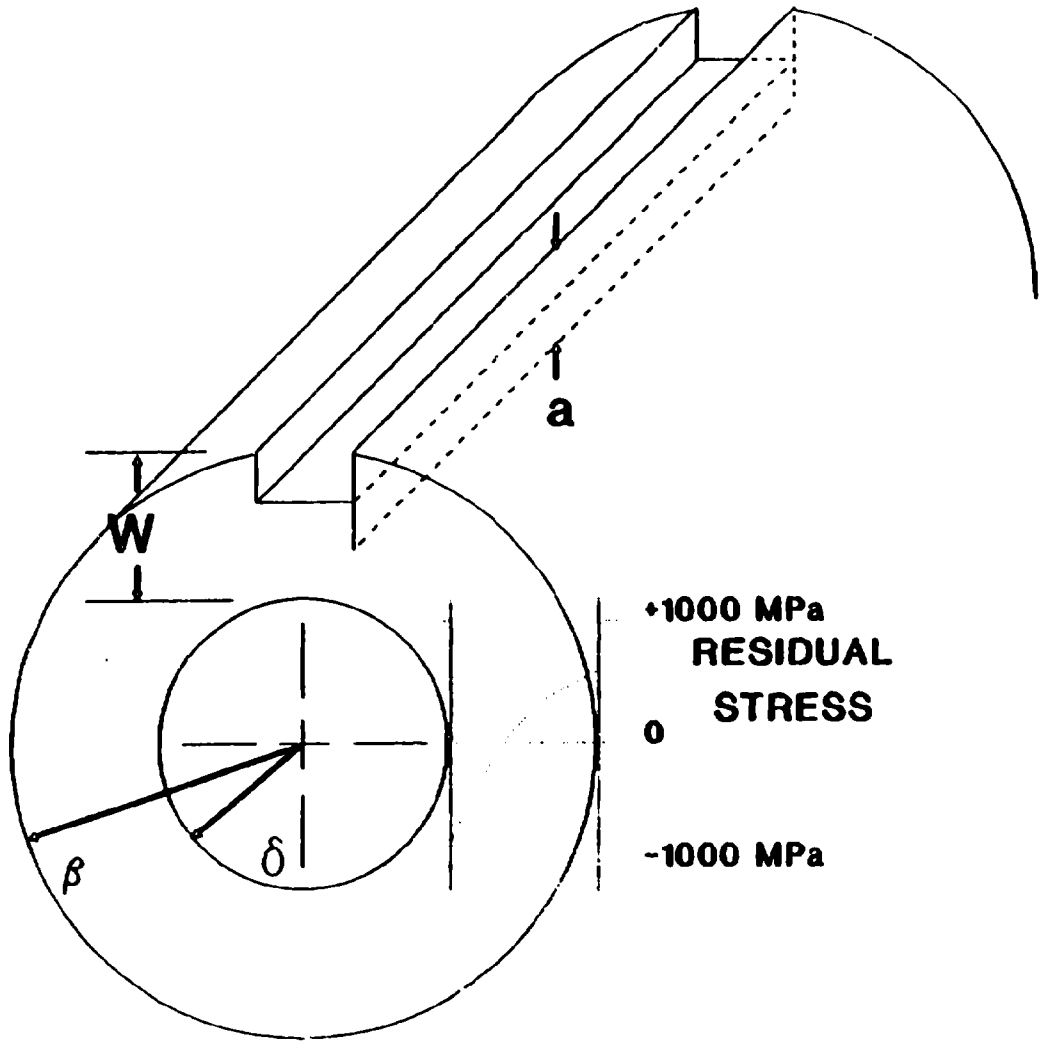

Figure 1. Sketch of overstrained tube configuration.

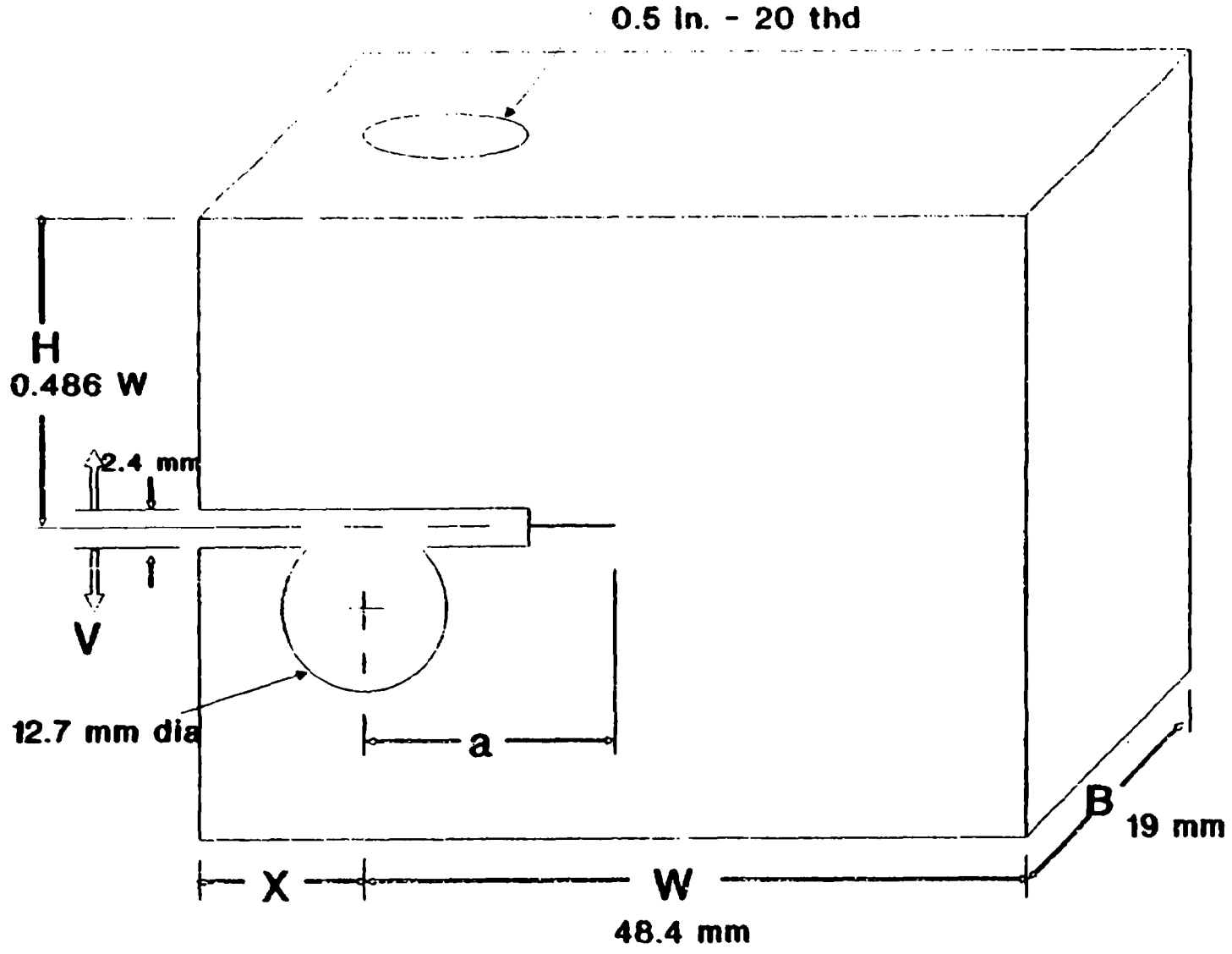

Figure 2. Bolt-loaded compact specimen for environmentally-controlled fracture tests.

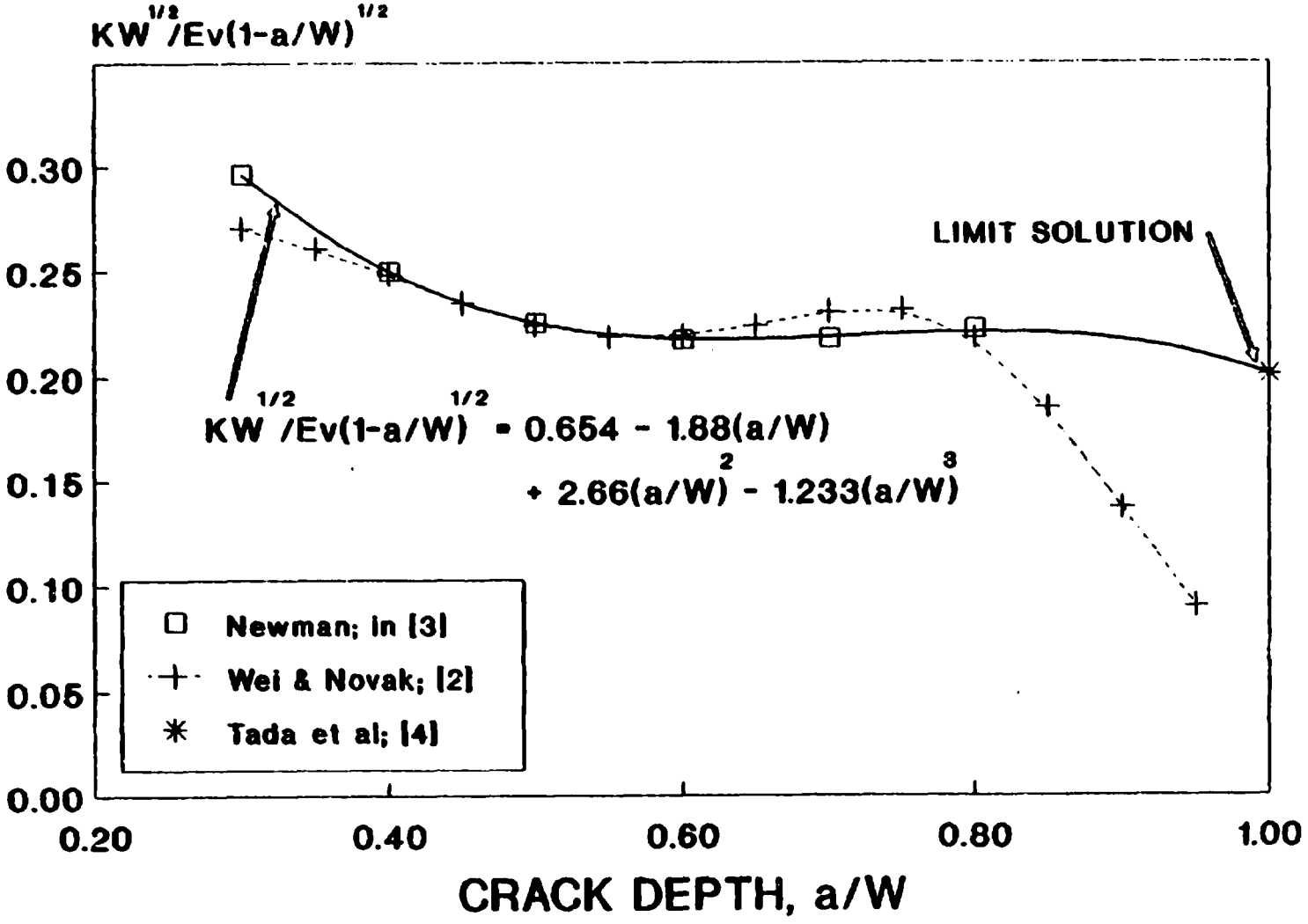

Figure 3. Comparison of K/v analyses for bolt-loaded compact specimen.

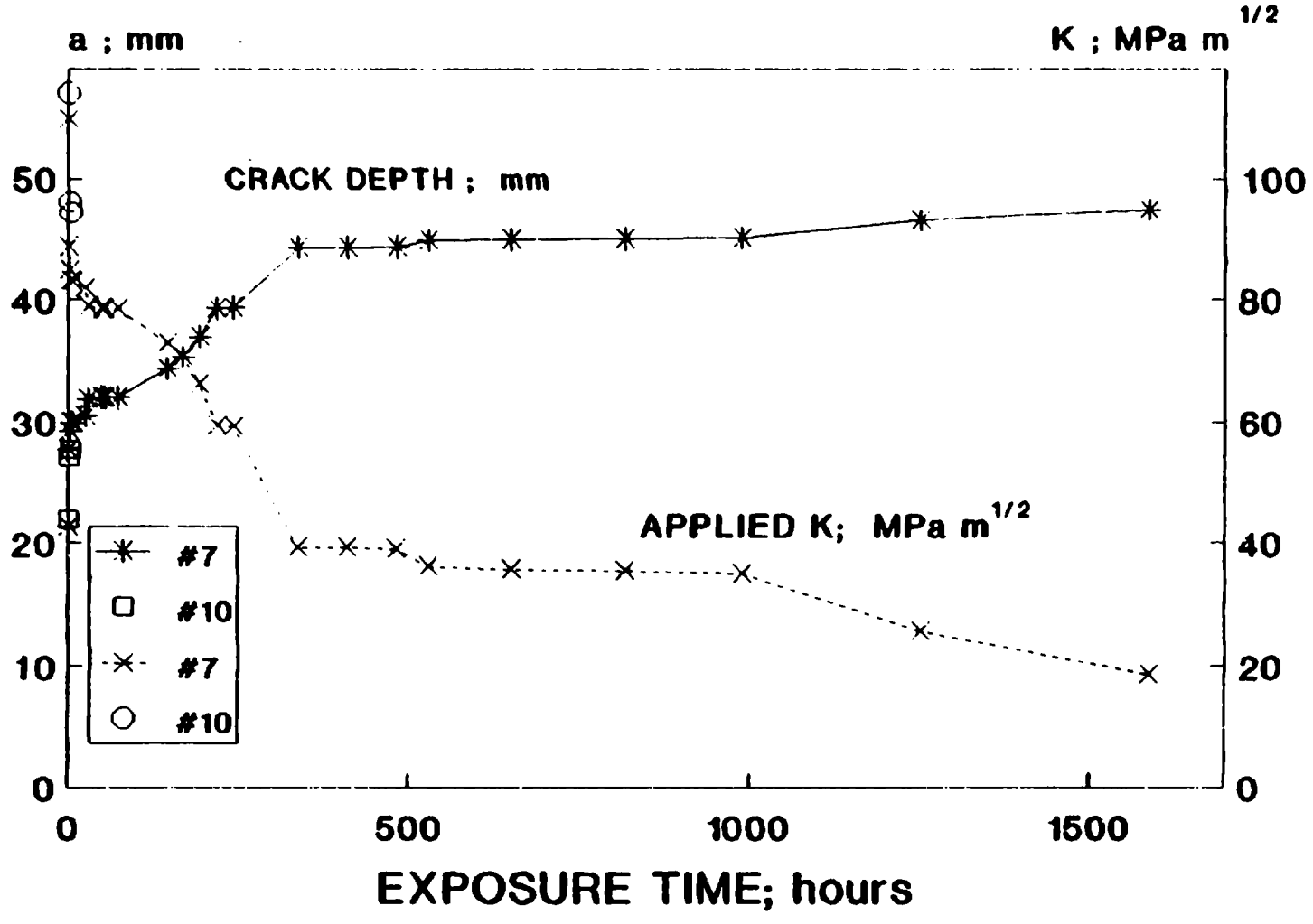

Figure 4. Crack growth and applied K for A723 steel exposed for 1600 hours to 50% H_2SO_4/50% H_3PO_4 at 54°C.

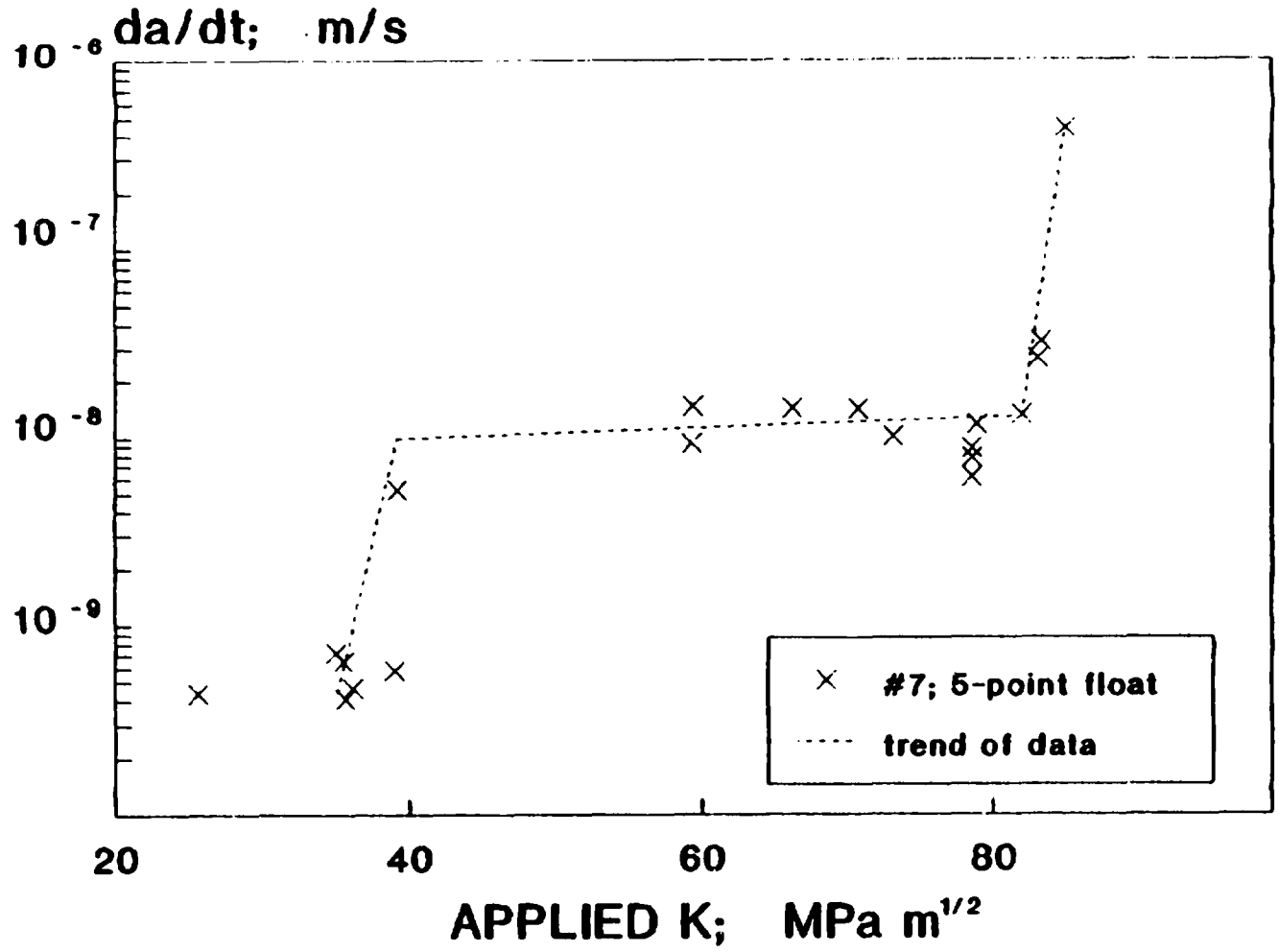

Figure 5. Crack growth rate versus applied K for A723 steel exposed to 50% H_2SO_4/50% H_3PO_4 at 54°C.

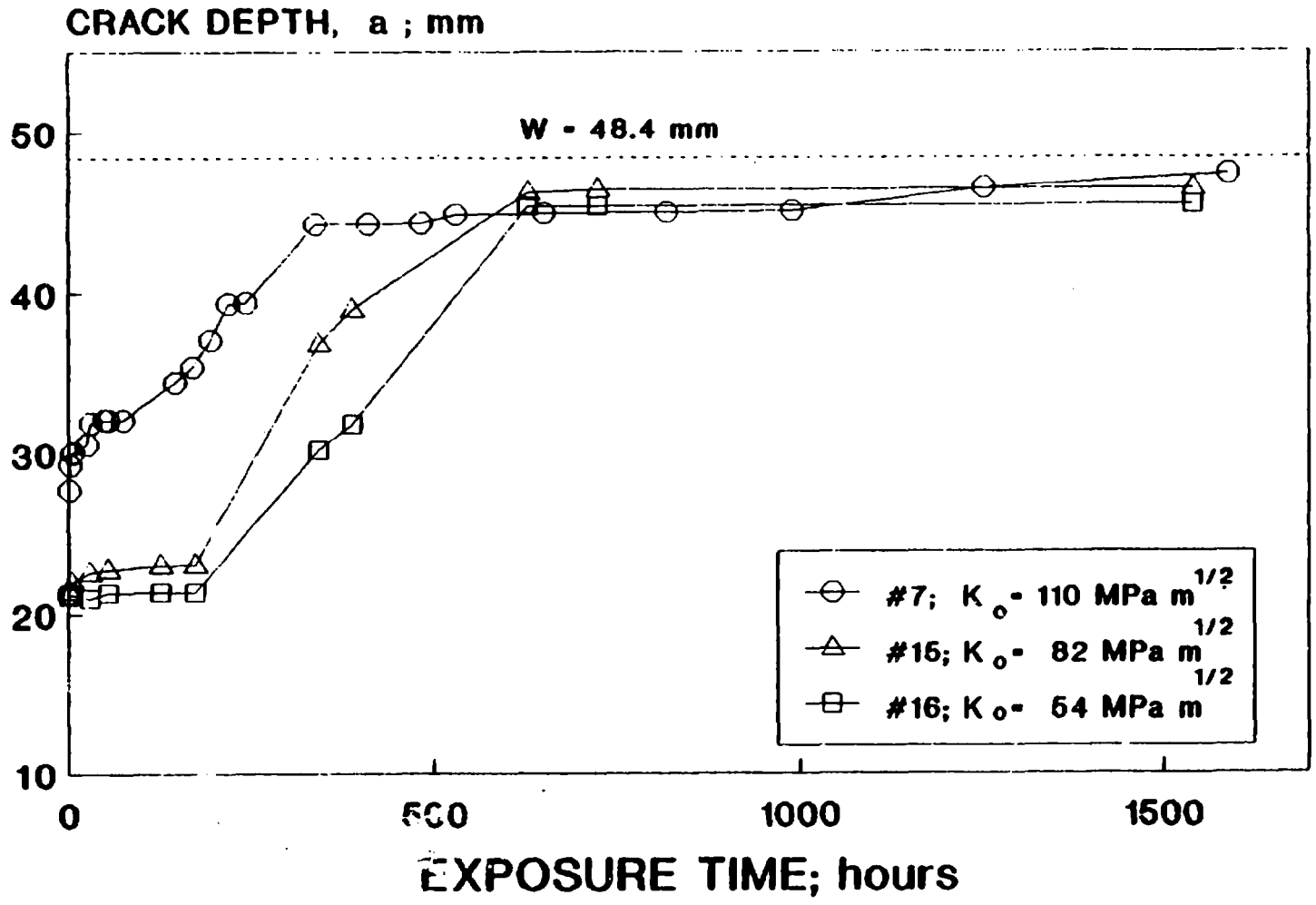

Figure 6. Crack growth for A723 steel exposed for 1600 hours to 50% H_2SO_4/50% H_3PO_4 at 54°C with various initial applied K values.

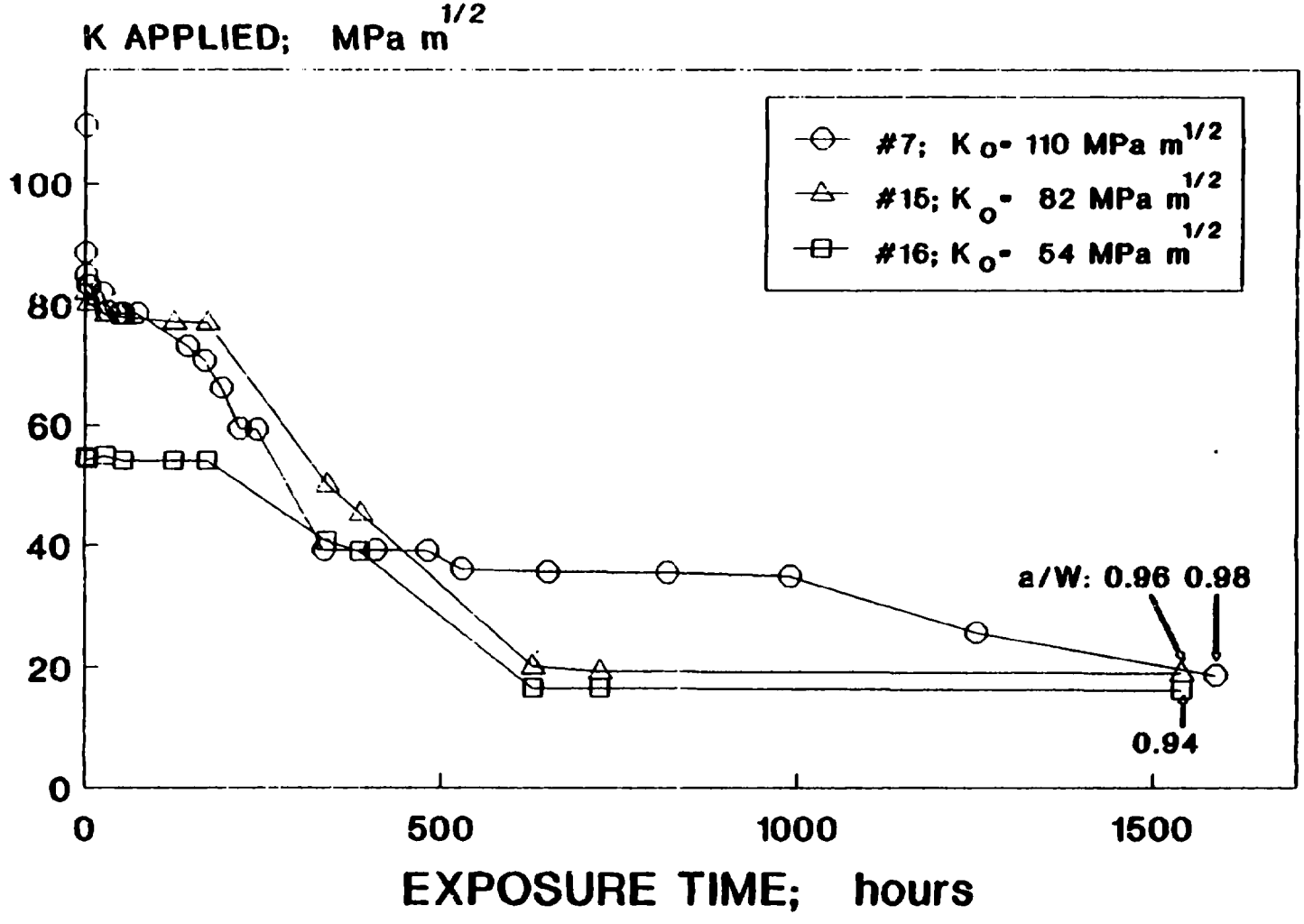

Figure 7. Applied K for A723 steel exposed for 1600 hours to 50% H_2SO_4/50% H_3PO_4 at 54°C with various initial applied K values.

[a]

macrophoto of specimen #7 (3.2X)

[b]

SEM fractograph of specimen #10 (44X)

Figure 8. Optical and SEM fractographs of A723 steel exposed for 1600 hours to 50% H_2SO_4/50% H_3PO_4 at 54°C.

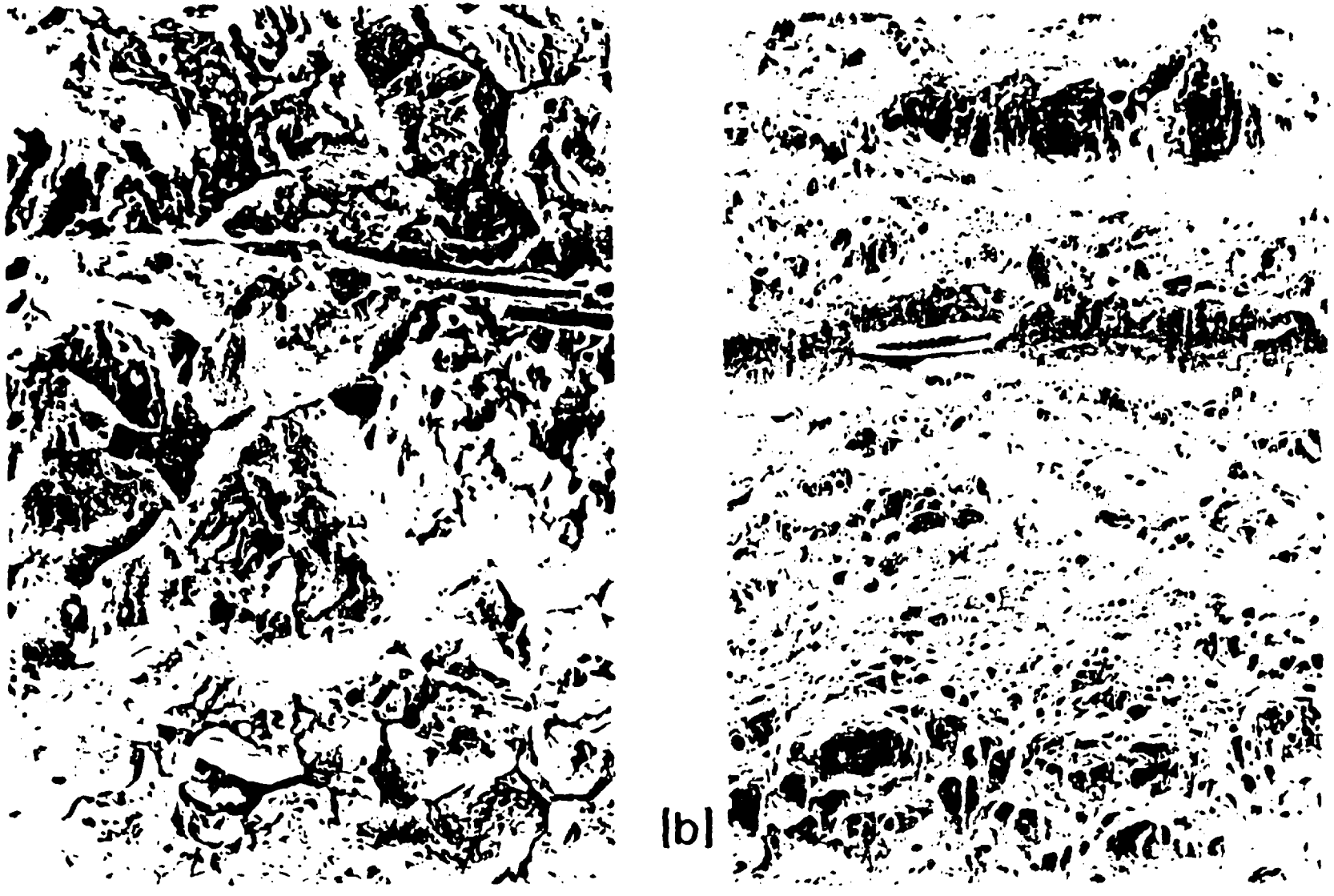

area of apparent environmental cracking, 2 mm ahead of notch

area of apparent fast cracking, 7 mm ahead of notch

Figure 9. SEM fractographs of failed A723 steel tube exposed to 50% H_2SO_4/50% H_3PO_4 at 54°C and other environments (1000X).

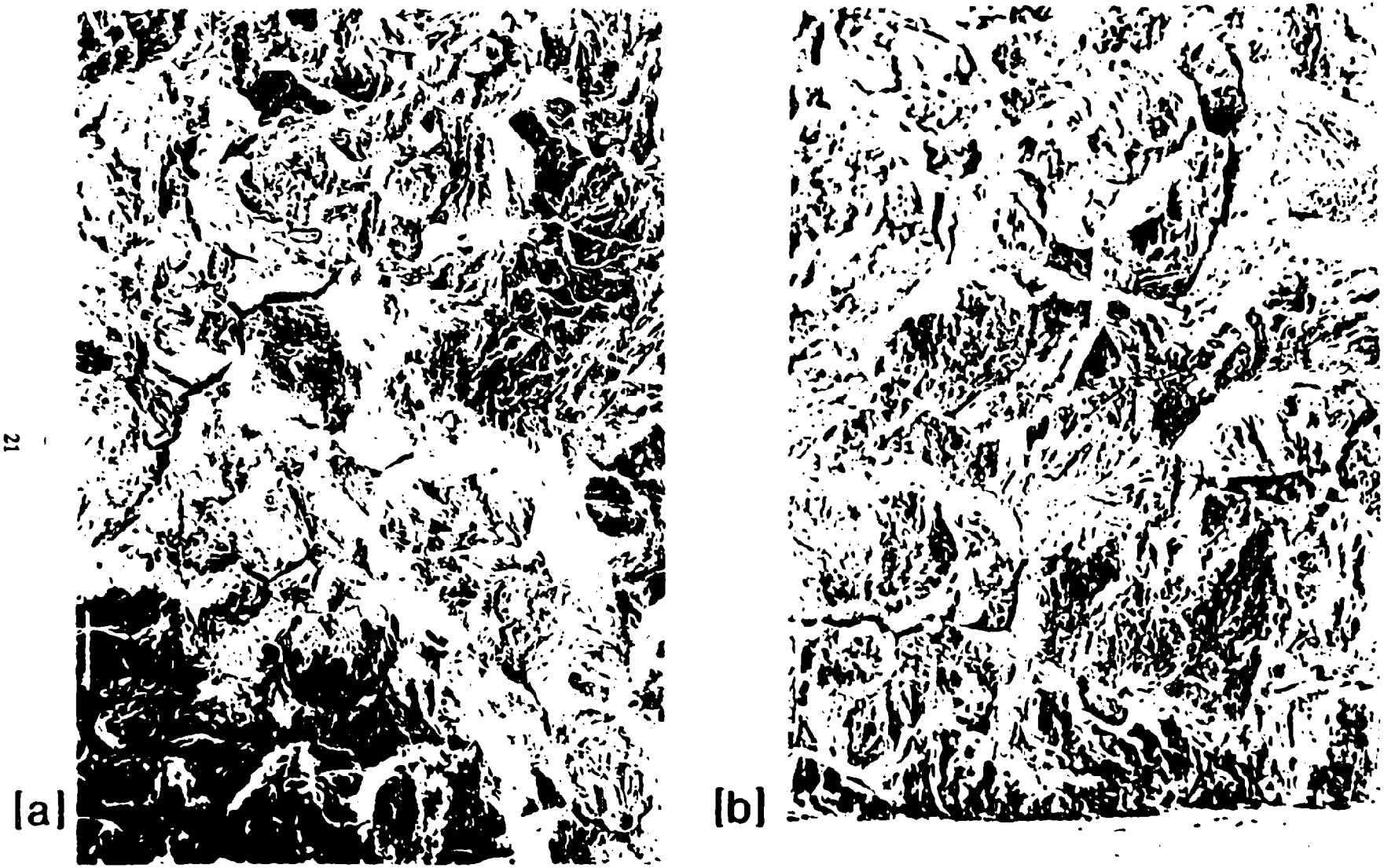

specimen #10: area near the end of apparent environmental cracking

specimen #17: area adjacent to notch

Figure 10. SEM fractographs of A723 steel exposed to 50% H_2SO_4/50% H_3PO_4 at 54°C (1000x).

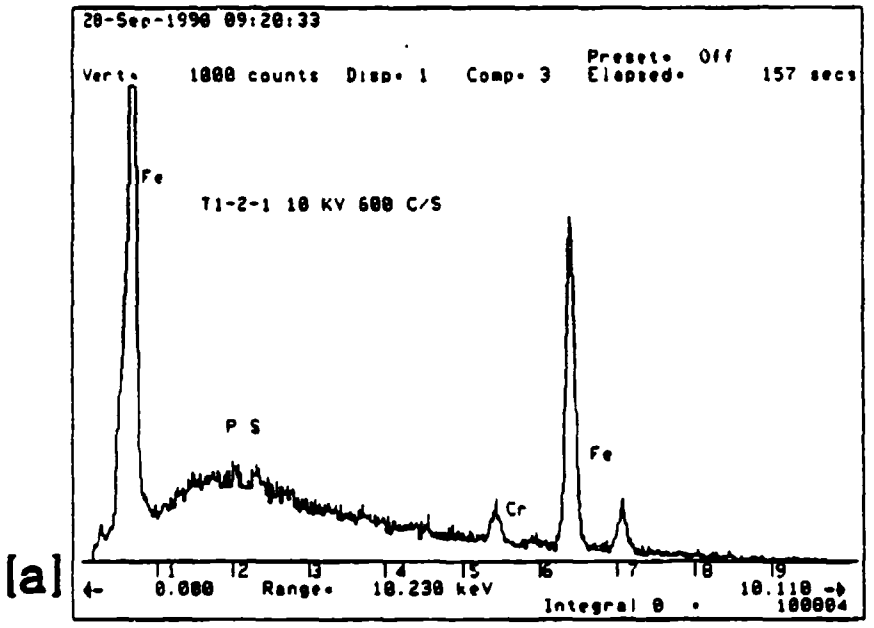

[a]

failed tube: area of apparent environmental cracking but relatively free of corrosion products

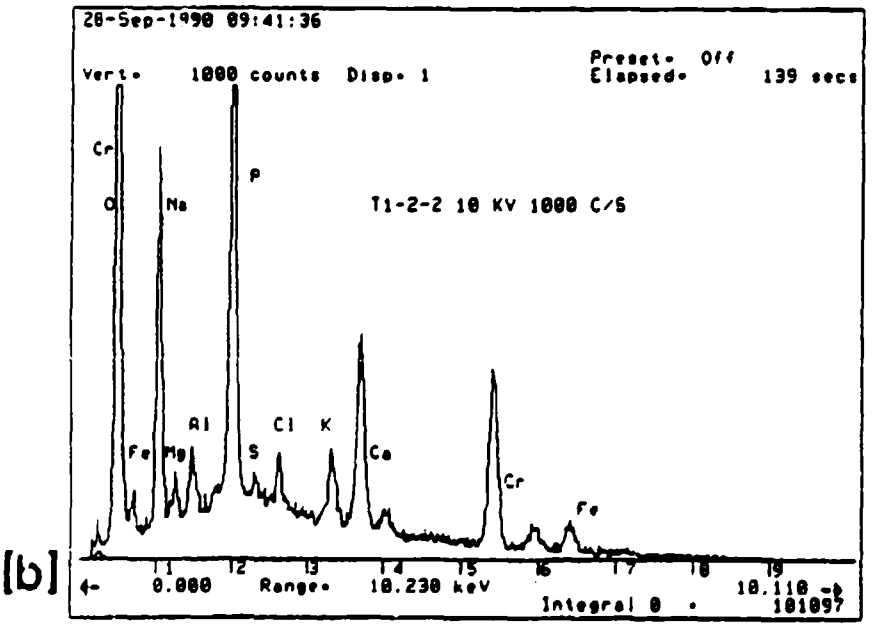

[b]

failed tube: area of apparent environmental cracking with corrosion products

Figure 11. Energy dispersive x-ray spectra of A723 steel fracture surfaces subjected to various environments.

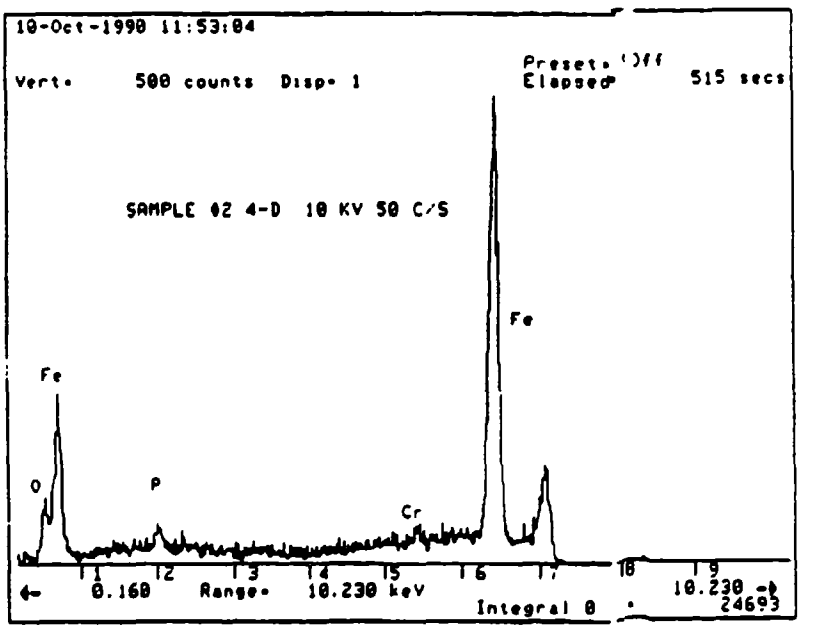

[c]

specimen #10: area of apparent environmental cracking but relatively free of corrosion products

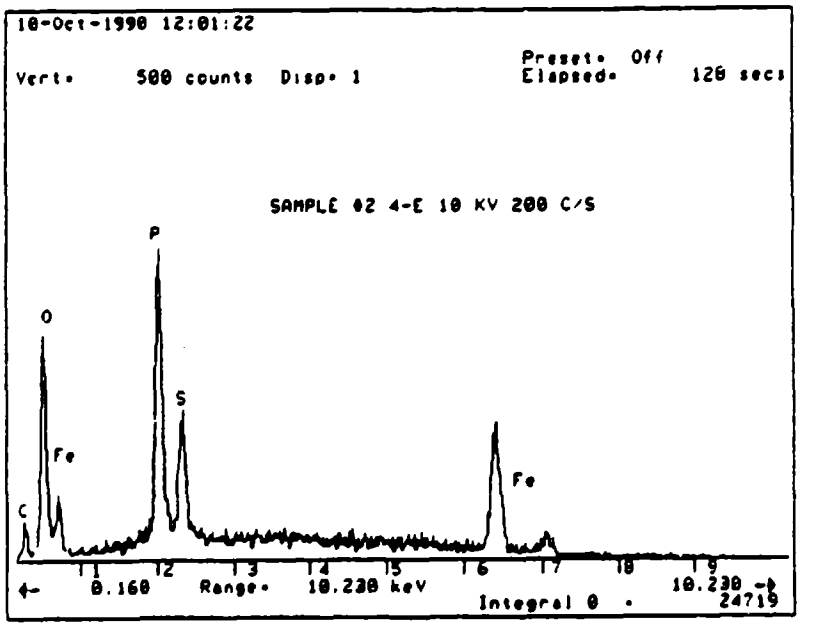

[d]

specimen #10: area of apparent environmental cracking with corrosion products

Figure 11. Continued

TECHNICAL REPORT INTERNAL DISTRIBUTION LIST

	NO. OF COPIES
CHIEF, DEVELOPMENT ENGINEERING DIVISION	
ATTN: SMCAR-CCB-DA	1
-DC	1
-DI	1
-DR	1
-DS (SYSTEMS)	1
CHIEF, ENGINEERING SUPPORT DIVISION	
ATTN: SMCAR-CCB-S	1
-SD	1
-SE	1
CHIEF, RESEARCH DIVISION	
ATTN: SMCAR-CCB-R	2
-RA	1
-RE	1
-RM	1
-RP	1
-RT	1
TECHNICAL LIBRARY ATTN: SMCAR-CCB-TL	5
TECHNICAL PUBLICATIONS & EDITING SECTION ATTN: SMCAR-CCB-TL	3
OPERATIONS DIRECTORATE ATTN: SMCWV-ODP-P	1
DIRECTOR, PROCUREMENT DIRECTORATE ATTN: SMCWV-PP	1
DIRECTOR, PRODUCT ASSURANCE DIRECTORATE ATTN: SMCWV-QA	1

NOTE: PLEASE NOTIFY DIRECTOR, BENET LABORATORIES, ATTN: SMCAR-CCB-TL, OF ANY ADDRESS CHANGES.

TECHNICAL REPORT EXTERNAL DISTRIBUTION LIST

	NO. OF COPIES
ASST SEC OF THE ARMY RESEARCH AND DEVELOPMENT ATTN: DEPT FOR SCI AND TECH THE PENTAGON WASHINGTON, D.C. 20310-0103	1
ADMINISTRATOR DEFENSE TECHNICAL INFO CENTER ATTN: DTIC-FDAC CAMERON STATION ALEXANDRIA, VA 22304-6145	12
COMMANDER US ARMY ARDEC ATTN: SMCAR-AEE	1
SMCAR-AES, BLDG. 321	1
SMCAR-AET-O, BLDG. 351N	1
SMCAR-CC	1
SMCAR-CCP-A	1
SMCAR-FSA	1
SMCAR-FSM-E	1
SMCAR-FSS-D, BLDG. 94	1
SMCAR-IMI-I (STINFO) BLDG. 59 PICATINNY ARSENAL, NJ 07806-5000	2
DIRECTOR US ARMY BALLISTIC RESEARCH LABORATORY ATTN: SLCBR-DD-T, BLDG. 305 ABERDEEN PROVING GROUND, MD 21005-5066	1
DIRECTOR US ARMY MATERIEL SYSTEMS ANALYSIS ACTV ATTN: AMXSY-MP ABERDEEN PROVING GROUND, MD 21005-5071	1
COMMANDER HQ, AMCCOM ATTN: AMSMC-IMP-L ROCK ISLAND, IL 61299-6000	1
COMMANDER ROCK ISLAND ARSENAL ATTN: SMCRI-ENM ROCK ISLAND, IL 61299-5000	1
DIRECTOR US ARMY INDUSTRIAL BASE ENGR ACTV ATTN: AMXIB-P ROCK ISLAND, IL 61299-7260	1
COMMANDER US ARMY TANK-AUTMV R&D COMMAND ATTN: AMSTA-DDL (TECH LIB) WARREN, MI 48397-5000	1
COMMANDER US MILITARY ACADEMY ATTN: DEPARTMENT OF MECHANICS WEST POINT, NY 10996-1792	1
US ARMY MISSILE COMMAND REDSTONE SCIENTIFIC INFO CTR ATTN: DOCUMENTS SECT, BLDG. 4484 REDSTONE ARSENAL, AL 35898-5241	2
COMMANDER US ARMY FGN SCIENCE AND TECH CTR ATTN: DRXST-SD 220 7TH STREET, N.E. CHARLOTTESVILLE, VA 22901	1
COMMANDER US ARMY LABCOM MATERIALS TECHNOLOGY LAB ATTN: SLCMT-IML (TECH LIB) WATERTOWN, MA 02172-0001	2

NOTE: PLEASE NOTIFY COMMANDER, ARMAMENT RESEARCH, DEVELOPMENT, AND ENGINEERING CENTER, US ARMY AMCCOM, ATTN: BENET LABORATORIES, SMCAR-CCB-TL, WATERVLIET, NY 12189-4050, OF ANY ADDRESS CHANGES.

TECHNICAL REPORT EXTERNAL DISTRIBUTION LIST (CONT'D)

	NO. OF COPIES
COMMANDER US ARMY LABCOM, ISA ATTN: SLCIS-IM-TL 2800 POWDER MILL ROAD ADELPHI, MD 20783-1145	1
COMMANDER US ARMY RESEARCH OFFICE ATTN: CHIEF, IPO P.O. BOX 12211 RESEARCH TRIANGLE PARK, NC 27709-2211	1
DIRECTOR US NAVAL RESEARCH LAB ATTN: MATERIALS SCI & TECH DIVISION CODE 26-27 (DOC LIB) WASHINGTON, D.C. 20375	1 1
DIRECTOR US ARMY BALLISTIC RESEARCH LABORATORY ATTN: SLCBR-IB-M (DR. BRUCE BURNS) ABERDEEN PROVING GROUND, MD 21005-5066	1
COMMANDER AIR FORCE ARMAMENT LABORATORY ATTN: AFATL/MN EGLIN AFB, FL 32542-5434	1
COMMANDER AIR FORCE ARMAMENT LABORATORY ATTN: AFATL/MNF EGLIN AFB, FL 32542-5434	1
MIAC/CINDAS PURDUE UNIVERSITY 2595 YEAGER ROAD WEST LAFAYETTE, IN 47905	1

NOTE: PLEASE NOTIFY COMMANDER, ARMAMENT RESEARCH, DEVELOPMENT, AND ENGINEERING CENTER, US ARMY AMCCOM, ATTN: BENET LABORATORIES, SMCAR-CCB-TL, WATERVLIET, NY 12189-4050, OF ANY ADDRESS CHANGES.